Korean J. Chem. Eng., 39(9), 2263-2274 (2022)
DOI: 10.1007/s11814-022-1173-5
pISSN: 0256-1115
eISSN: 1975-7220

REVIEW PAPER

A short review on hydrophobic pervaporative inorganic membranes for ethanol/water separation applications

Hyung-Ju Kim*,†, Sung-Jun Kim*, Keunyoung Lee*, and Richard I. Foster*,,†**

*Decommissioning Technology Research Division, Korea Atomic Energy Research Institute, 989-111 Daedeok-daero, Yuseong-gu, Daejeon 34057, Korea
**Nuclear Research Institute for Future Technology and Policy, Seoul National University, 1 Gwanak-ro, Gwanak-gu, Seoul 08826, Korea
(*Received 1 February 2022 • Revised 5 May 2022 • Accepted 11 May 2022*)

Abstract−Inorganic based membranes are promising candidates for a variety of applications, including adsorption and separation due to their large surface area, high pore volume, tunable structure, and strong resistance against aggressive operation conditions, such as high temperature and pressure. Many research groups have investigated zeolite, micro- or mesoporous silica, and hybrid materials (organic and inorganic materials) as advanced membrane configurations in liquid separation applications. Especially, hydrophobic inorganic membranes have potential to separate ethanol from aqueous solution via pervaporation, ultimately producing ethanol, but several important challenges such as reliable synthesis, fabrication, or functionalization are yet to be solved. More specifically, a novel, high throughput process for the fabrication of continuous and defect-free hydrophobic inorganic membranes is required. Then, functionalization of pore structures of the membrane, if necessary, is desirable in order to tailor even more advanced hydrophobic properties for ethanol. Finally, the separation characteristics and performance of inorganic membranes must be further investigated to implement in the industry. Herein, the synthesis and normalized separation performance of diverse hydrophobic inorganic membranes with respect to selective layer material basis, such as zeolite, functionalized mesoporous silica, and mixed matrix, are comprehensively reviewed and the future direction is presented with a focus on ethanol recovery.

Keywords: Ethanol/Water Separation, Hydrophobic Membrane, Mesoporous Silica, Mixed Matrix Membrane, Pervaporation, Zeolite

INTRODUCTION

Fossil resources are not regarded as sustainable, in part due to oil scarcity which leads to oil price rises, nor promising energy sources considering the environment [1]. Further, the utilization of fossil fuels is a major contributor to the increasing concentration of carbon dioxide (CO_2) in the atmosphere resulting in worldwide climate change [2]. For these reasons, many sustainable and nature-friendly energy sources, such as solar and wind, have been getting attention [3]. Also, there is a great interest in the production of biofuel as a nature-friendly energy source, because it can be utilized and produced sustainably in the absence of CO_2 emission [4,5]. One of the most common types of biofuel is bioethanol. Bioethanol is an alcohol made via fermentation, mostly from carbohydrates produced in sugar or starch crops [6], and is widely used in various countries having plenty of these natural resources [7]. Thus, the efficient production of bioethanol is becoming increasingly important [8].

In bioethanol production plants, a significant portion of their total energy requirement (about 40%) is consumed for ethanol (EtOH)/water separation [9,10]. To obtain purified EtOH, ultimately biofuel, energy-efficient and profitable producing of EtOH from aqueous solution is imperative. The conventional fractionation, distillation, and adsorption technologies have been applied to produce high purity EtOH from the aqueous mixture [11]. However, such processes require substantial energy and cost [12]. Also, efficient separation of EtOH and water by distillation is not feasible because the mixture is an azeotrope [13], liquid mixtures with similar breakpoints [14], and liquid-liquid isomers [15]. To overcome these limitations, membrane separation is widely used as an alternative strategy for selectively and continuously separating EtOH from water [16]. EtOH selective hydrophobic membranes have been considered to replace other existing conventional processes, such as distillation, adsorption, and liquid-liquid extraction [17-19].

A wide range of materials have been utilized to synthesize selective membranes [20]. Fig. 1 shows membrane classifications by material. Membranes can be synthesized from polymers, inorganics, or their combination, so-called mixed matrix membranes (MMMs) [21]. The membranes are composed of a selective layer atop of a porous support. A structure suitable for the fields driven at high pressure should consist of a support providing mechanical strength and a thin separation layer to achieve good performance. The support layer should have a high throughput and almost no selective property, whereas the dense membrane layer is an active layer with the property of separating target mixtures. The selective layer should be thin enough to increase permeance, and it can be functionalized

†To whom correspondence should be addressed.
E-mail: hyungjukim@kaeri.re.kr, rifoster@snu.ac.kr

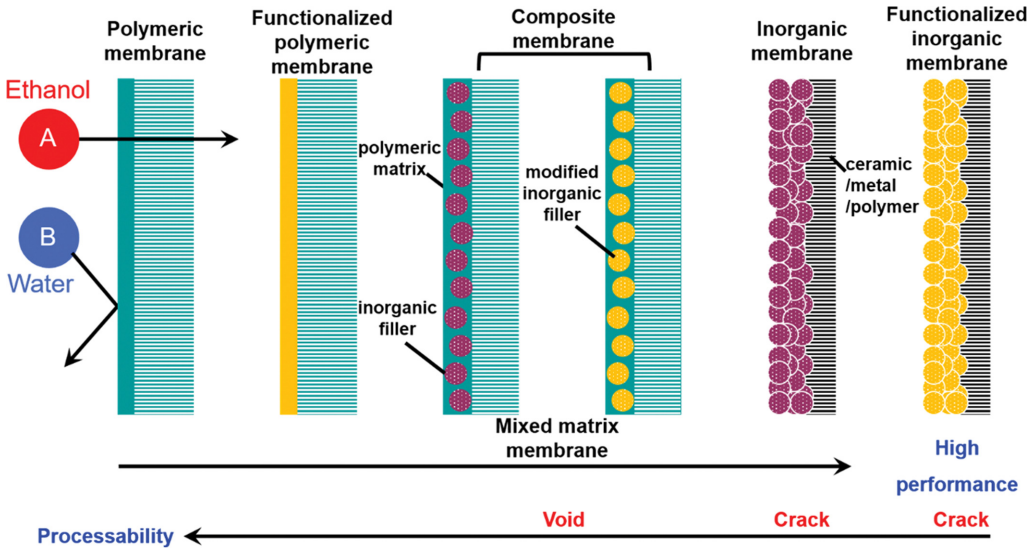

Fig. 1. Membrane classification by material.

or modified further to tailor target selectivity (i.e., the yellow active layer or inorganic fillers in Fig. 1). Membranes based on polymers or inorganic materials exhibit a trade-off between properties regarding separation performance. A polymeric membrane has high processability, but low performance compared with inorganic membranes. Conversely, inorganic membranes exhibit high performance and low processability due to the undesirable discontinuity and cracks in the membrane framework. Inorganic membranes composed of silica, alumina (Al_2O_3), or zeolite have a high solvent resistance, high-temperature stability and are free of swelling compared to other polymer membranes [22]. They also have powerful separation performance, high selectivity and permeability, because of their intrinsic surface properties and narrow pore size distributions [23]. Due to such superior features, inorganic separation membranes can be applied to a wide range of applications including EtOH/water separation with hydrophobic property [24].

There are various membrane-based liquid separation processes: ultrafiltration [25], nanofiltration [26], reverse osmosis [27] and forward osmosis [28]. Among the membrane-based separation or purification techniques reported in the literature, pervaporation (PV) is the most favorable technique for the application of EtOH/water separation [29], because it can operate under low feed pressures and ambient temperatures without any additional chemicals. Fundamentally, PV transport is not restricted by osmotic pressure, because the driving force for mass transfer over the membrane is served by lowering the chemical potential of the downstream permeate [20]. During the PV process, a membrane is placed in contact with an aqueous mixture, and the mixture undergoes a phase transformation from liquid to vapor while passing through the membrane layer [30]. Thus, PV is regarded as one of the simplest techniques for separation of azeotropic mixtures [23].

In this review, various hydrophobic inorganic membranes with different supports for EtOH recovery from aqueous solution are discussed, while membrane separation performance, with respect to commonly reported flux and separation factor, is compared. Then, the normalized membrane performance, such as permeance and selectivity, is computed with given information from literatures for direct comparison and useful selection of superior inorganic membranes. Thus, the effects of EtOH/water feed composition, various materials used in membrane synthesis, and operation conditions on PV membrane separation techniques are introduced, with proposals for the future direction of PV inorganic membranes being discussed.

BACKGROUND

PV is permselective evaporation, and the mechanism, so called solution-diffusion, consists of three steps: selective sorption of the target component, selective diffusion of the component through the membrane, and component desorption into a vapor phase on the permeate side [20]. As shown in Fig. 2, there are two different separation applications, depending on the feed composition and membrane property. When the concentration of the EtOH in an aqueous feed is low, PV permeates the EtOH through a hydrophobic membrane, the application covered in this review. Subsequently, water is recovered from the feed side, while the EtOH is collected on the permeate side. Conversely, for an EtOH based feedstock containing a relatively small amount of water, PV dehydrates the feed through a hydrophilic membrane (not being covered in this review). Then, the water and EtOH are recovered from permeate and feed sides, respectively.

Fig. 3 illustrates a laboratory scale PV system for flat film membranes. A chosen membrane is housed in the flat film module that remains in contact with the feed solution, while the selective layer faces toward the liquid mixture throughout the separation process. The membrane acts as a selective barrier between the two-phases (i.e., the liquid feed mixture and the vapor permeate). During the PV process, a vacuum is applied on the permeate side of the membrane, while the membrane feed side is kept at atmospheric pressure with proper stirring for homogenization of the mixture. The feed mixture evaporates while passing through the membrane with respect to the permeation affinity. The driving force in this phe-

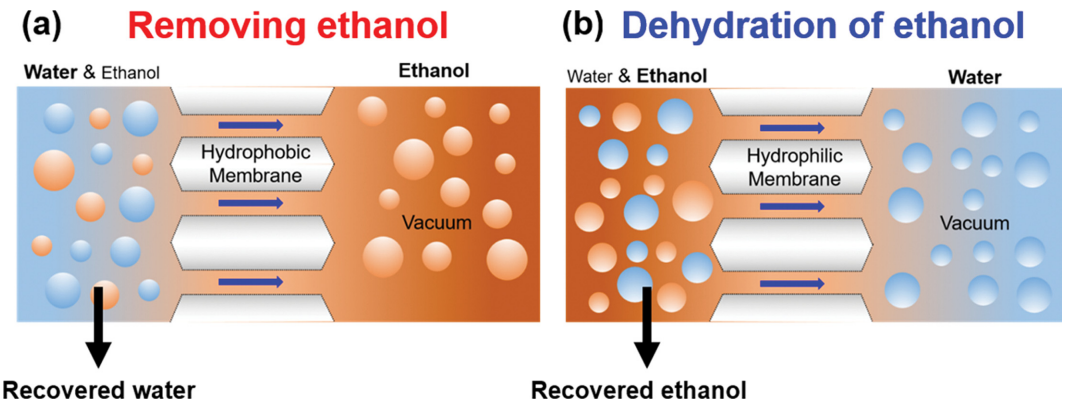

Fig. 2. Illustration of (a) removing ethanol and (b) dehydration from each feed mixture using hydrophobic and hydrophilic membranes.

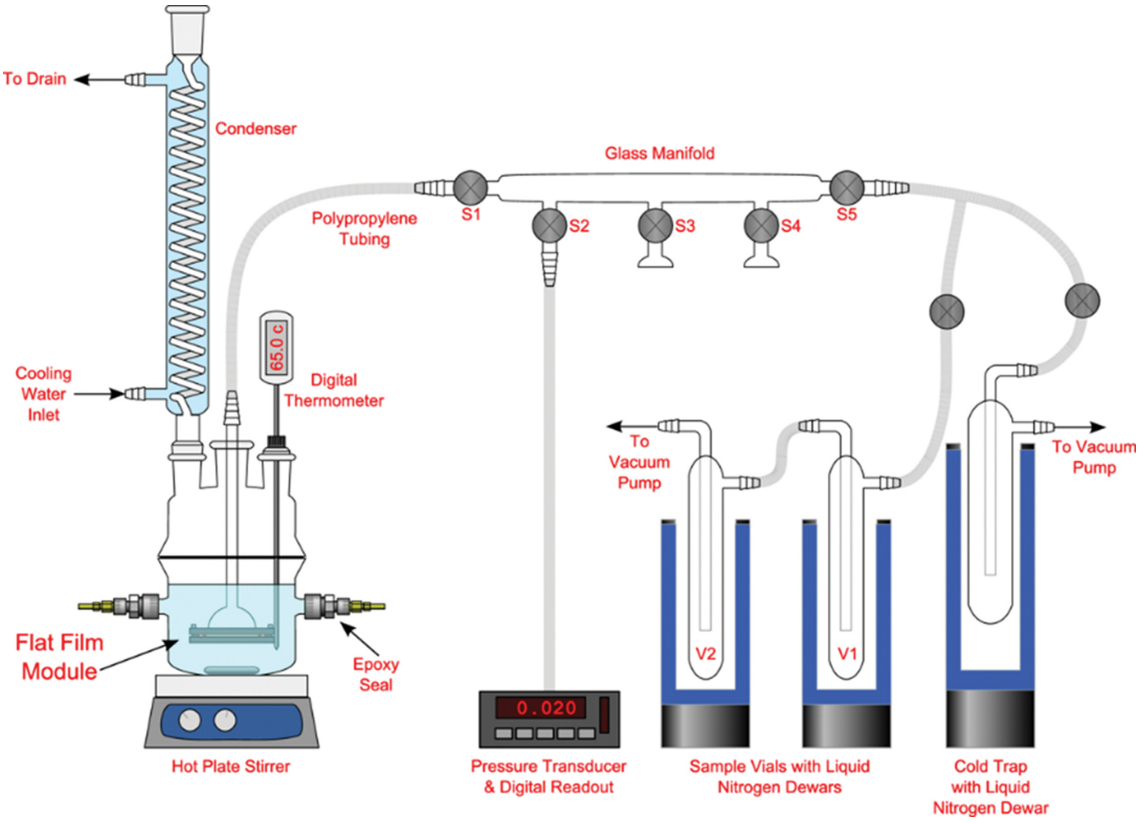

Fig. 3. Illustration of PV system with flat film membranes.

nomenon is the pressure differential between the feed and permeate [31]. As the PV process proceeds, the permeating liquid is completely vaporized and passes through the manifold. The vaporized liquid then condenses inside of collection vials which are maintained in thermal equilibrium with liquid nitrogen (77 K). Tunable variables for mass transfer such as the feed concentrations, pressure differential, operation time, and temperature can be controlled, while membrane properties such as surface nature, thickness, and exposed surface area can be optimized for enhanced separation performance.

For the quantitative experimental results, flux and separation factor are acquired from the PV process [32]. The flux, usually given as a mass flux, of component i (F_i) is described as Eq. (1):

$$F_i = \frac{y_i w}{A\Delta t} \tag{1}$$

where y_i is the mass fraction of the permeate, w is the total mass of permeate, A is the exposed surface area of the membrane, and Δt is operation time. A separation factor ($\beta_{i/j}$) can be described as Eq. (2):

$$\beta_{i/j} = \frac{y_i/y_j}{x_i/x_j} \tag{2}$$

where x_i and x_j are the mass fractions of the component i and j

in the feed; y_i and y_j are the mass fractions of component i and j in the permeate. Many researchers superficially report PV membrane performance in terms of mass fluxes in Eq. (1) and separation factors in Eq. (2). However, these values significantly depend on the properties of the synthesized membrane and operating conditions such as feed concentration, feed temperature, and differential pressure. Thus, direct comparison of the PV data obtained under various conditions with different membranes is impossible. Since permeability, permeance, and selectivity are including the operating conditions as well as intrinsic properties of the membrane itself, converting performance data reported in various literatures to a normalized form is necessary in order to equally compare the separation performance of PV membranes. Baker et al. proposed a method for calculating permeability, permeance, and selectivity to express the performance of PV membranes [33]. Membrane permeability (P_i) is a normalized term reflecting membrane thickness and driving forces, here pressure difference, as given by Eq. (3):

$$P_i = \frac{J_i l}{\Delta p_i} \tag{3}$$

where J_i is the molar flux of component i, calculated by dividing mass flux (F_i) with molecular weight, l is the membrane thickness, and Δp_i is pressure difference between the feed and permeate. The pressure difference can be calculated as follows based on vapor liquid equilibrium, Eq. (4):

$$\Delta p_i = \gamma_i x_i p_i^{sat} - y_i p_p \tag{4}$$

where γ_i is the activity coefficient, p_i^{sat} is the saturated vapor pressure, and p_p is the permeate pressure. If the membrane thickness is not reported in the literature, permeance ($P_i\, l^{-1}$) can be alternatively used as shown in Eq. (5).

$$\frac{P_i}{l} = \frac{J_i}{\gamma_i x_i p_i^{sat} - y_i p_p} \tag{5}$$

Permeability is expressed in Barrer (1 Barrer = 3.35×10^{-16} mol m m^{-2} s^{-1} Pa^{-1}), while permeance is given as GPU (gas permeation unit, 1 GPU = 3.35×10^{-10} mol m^{-2} s^{-1} Pa^{-1}). Membrane selectivity ($\alpha_{i/j}$), a dimensionless number described in Eq. (6), exhibiting a more accurate meaning of the selective property than separation factor, can be calculated by the ratio of the permeabilities or permeances of components i and j.

$$\alpha_{i/j} = \frac{P_i}{P_j} = \frac{P_i/l}{P_j/l} \tag{6}$$

This proposed method by Baker et al. normalizes various operational conditions of PV and membrane thickness, and enables the separation performance of diverse PV processes to be directly compared.

HYDROPHOBIC INORGANIC PV MEMBRANES

Several types of hydrophobic inorganic PV membranes have been developed to separate EtOH/water, including zeolite, functionalized mesoporous silica, and MMMs. Such inorganic membranes have hydrophobic surfaces and pores which preferentially

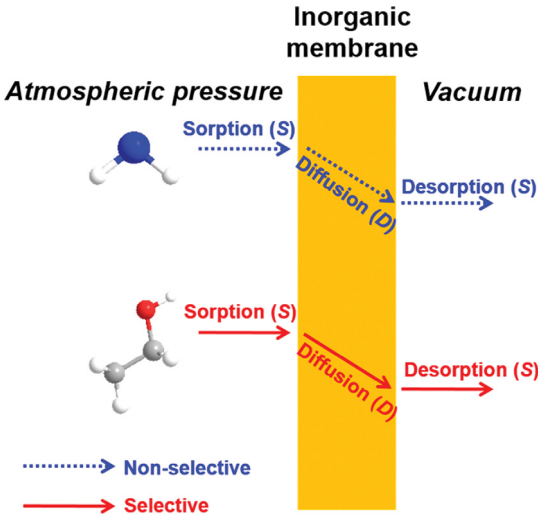

Fig. 4. The PV retention mechanism of EtOH/water when hydrophobic inorganic membrane is used.

sorb EtOH, indicated by relatively higher heat of adsorption on EtOH while lower for water as shown in Fig. 4 [23]. This enables the EtOH transport through the hydrophobic inorganic membranes as solution-diffusion mechanism while repelling water [30]. Hydrophobic inorganic membrane separations have been successful despite the fact that a water molecule (kinetic diameter of 0.296 nm) is smaller than an EtOH molecule (kinetic diameter of 0.430 nm). This is because the transport is more dependent on solubility, not diffusivity, tailored by surface property [23]. Membrane performance is typically reported in the form of separation factor and mass flux. The extensive range of available data has been collated, analyzed and categorized on a per selective layer material basis.

1. Zeolite Membranes

Zeolites are hydrated microporous (<2 nm) aluminosilicates with a uniform crystal structure [34] which have value for catalysis and separations due to their adsorption property [35]. At the molecular level, gas or liquid molecules can easily adsorb and diffuse through the large surface area from micropores of zeolites [36]. Zeolite membranes can be synthesized by various methods to take advantage of particular adsorption and diffusion properties in separation [37]. Also, zeolite membranes have high chemical resistance and thermal stability compared to polymeric membranes [38]. Thus, zeolite membranes have received much attention as one of the promising candidates for EtOH/water PV separation [39]. Furthermore, the robust support materials (α-Al_2O_3, stainless steel (SS), and mullite tube, etc.) with diverse configurations (flat and tubular) providing mechanical strength to the zeolite membrane, are an important factor because they greatly affect the quality of the membrane. Therefore, researchers have investigated the effects of different support materials on the zeolite membranes [40-43].

Zeolites are chosen for optimal performance depending on the concentration of EtOH in the feed and the operating conditions such as temperature and pressure [44]. Kuhn et al. prepared multichannel defect-free silica rich MFI membranes for removal of 16 wt% EtOH/water [45]. They activated pores of MFI membrane on an asymmetric α-Al_2O_3 monolithic support through three differ-

ent ways: calcination (M1), ozonication (M2), and calcination after ozonication (M2c). The separation factors were 145, 204, and 107 with total flux of 0.36 kg m^{-2} h^{-1}, 0.19 kg m^{-2} h^{-1}, and 0.57 kg m^{-2} h^{-1} for M1, M2, and M2c under different temperatures, respectively. Since ozonication allows for detemplation to occur at 473 K, a much lower temperature than calcination, silanol groups in the zeolite structure are retained, which results in M2 showing a higher separation factor and lower flux. According to additional research by Kuhn et al., the amount of silanol group in ozonicated silicalite-1 is much higher than calcined silicalite-1 [46]. Additionally, the ozonication reduces the chance of crack formation coming from thermal stresses. Thus, the separation factor of the M2 was higher than M1 and M2c, because the calcination temperature causes deterioration of membrane structure.

Substitution of tri- and tetravalent elements, such as Al, Fe, B, and Ge etc., by in situ crystallization was also carried out to improve the performance of zeolite membranes. Tuan et al. prepared a substituted ZSM-5 membrane on a porous SS support, while a silicalite-1 membrane was prepared separately for comparison. Then, PV tests were performed for 5 wt% EtOH/water at 298 K [47]. Incorporating tri- and tetravalent elements into a zeolite structure can adjust zeolite pore sizes, highly affecting the selectivity and flux. Also, this treatment can alter the hydrophobicity of the zeolite. ZSM-5 membranes were produced with a Si/(Al, Fe, B, Ge) ratio of 100 on an SS support using alkali free synthesis gel. In their previous study, even if most conventional zeolite membranes had been synthesized by sodium hydroxide [48-51], Al-ZSM-5 membrane synthesized from alkali-free gels had a good separation performance for liquid mixtures other than EtOH [52]. The separation factor of the Ge-ZSM-5 membrane was highest (29) among other substituted ZSM-5 (less than 10) and silicalite-1 membranes (10). Surprisingly, the total flux and permeance of Ge-ZSM-5 were also superior to other membranes. Since Ge has the smallest diameter among the substitution elements, the highest degree of substitution was acquired in the membrane. The additional water adsorption study for Ge-ZSM-5 crystal also supports enhanced hydrophobicity of the membrane [53]. In another research, Sano et al. investigated the effect of support materials on membrane performance by hydrothermal synthesis of silicalite membranes on porous sintered SS and the Al_2O_3 disk with an average pore diameter of 0.5-2 μm. The PV separation on a 4.4 wt% EtOH/water was carried out at 303 K. For silicalite membranes on a sintered SS support, the separation factor and total flux were 58 and 0.22 kg m^{-2} h^{-1}, whereas a silicalite membrane on an Al_2O_3 support has a lower separation factor of 5.2 and flux of 0.19 kg m^{-2} h^{-1}, which stands for SS provides better support than Al_2O_3 for silicalite membrane [54]. On the other hand, B-ZSM-5 membrane was synthesized on α-Al_2O_3 coated SiC multi-channel monolith supports to take advantage of the larger surface-to-volume ratio of the monolith [55], and effectively removed EtOH from the aqueous mixture by PV across a temperature range of 303-333 K. The best performance of separation factor and flux for 5 wt% EtOH/water was 31 and 0.16 kg m^{-2} h^{-1}, respectively, at 333 K. In particular, the flux is quite comparable with the same B-ZSM-5 membrane on an SS tube, which indicates that the SiC based monolith, a potentially more practical platform, is feasible.

Among various types of zeolite, silicalite is frequently used for membrane synthesis because of its high flux and selectivity for EtOH separation from aqueous solutions when the zeolite layer is grown normal to the surface of the support [56]. Lin et al. synthesized silicalite membranes on α-Al_2O_3 by a single hydrothermal method. Silicalite powder and tetraethyl orthosilicate (TEOS) were used as a silica source for membranes. For α-Al_2O_3 support, the highest separation factor and flux were 89 and 1.8 kg m^{-2} h^{-1}, testing PV for a 5 wt% EtOH/water at 333 K [57]. This is because (1) Al dissolved from α-Al_2O_3 support incorporated into the zeolite layer and (2) silicalite powder and TEOS can increase the Si/Al ratio. Thus, the selective layer of the membrane is denser because the silicalite powder provides the nucleation site and TEOS affects the crystal growth. This indicates that both the support material and silica source affect the membrane performance as well as the properties of the selective layer. For the expansion, Lin et al. prepared silicalite membranes on a mullite tube by in situ crystallization (unseeded) and compared to the same membrane on α-Al_2O_3 tube or seeded mullite tube [58]. The silicalite membrane produced by in situ crystallization on mullite tube using colloidal silica showed the EtOH separation factor of 106 and flux of 0.9 kg m^{-2} h^{-1} in 5 wt% EtOH/water at 333 K. However, the same membrane prepared on α-Al_2O_3 tube and seeded mullite tube had reduced separation factors of 85 and 65, and compensated flux was increased up to 1.22 kg m^{-2} h^{-1} and 1.28 kg m^{-2} h^{-1}, respectively. From electron microscopy analysis of silicalite membranes on α-Al_2O_3 and seeded mullite tubes, dome-like defects were observed in the membrane layers. Additionally, they found that a uniform seed layer could not be formed because of the large silicalite powder size (up to 4 μm) and rough surface of the mullite support. On the other hand, surface and cross section morphology of the silicalite membrane prepared by in situ crystallization on mullite tube using colloidal silica showed full coverage and random orientation of the crystal layer. That is, the property of the support affected the morphology of the membrane, ultimately leading to influencing the membrane performance. Chen et al. tested a high performance silicalite-1 membrane synthesized on silica tubes by a newly developed method called "solution filling" (SF) [59]. Silica tube supports were filled with a viscous mixed solution including water and glycerol. PV showed separation factor of 66 and flux of 1.49 kg m^{-2} h^{-1} for 3 wt% EtOH/water at 333 K. These were higher than the performance of a membrane synthesized without the SF. The glycerol, permeated through the tube and acted as a template, increasing the number of nuclei on the silica tube, which resulted in a smaller zeolite crystal. Thus, the size reduction of the zeolite leads to the increased quantity of intercrystalline pathways, and results in significantly increasing the membrane flux while maintaining a marginal separation factor.

In Table 1, the reported EtOH/water PV separation performance using zeolite membranes is summarized with regard to the type of zeolite and support, feed composition, operation temperature, separation factor, and total flux. Then, permeance and selectivity were further computed with the aforementioned method. Also, the reported unit of flux was converted to L m^{-2} h^{-1} (LMH), which is more familiar value in the liquid separation membrane community. Additionally, the water contact angle, a measurement of the hydrophobicity of the inorganic membranes, was surveyed and reported.

Table 1. EtOH/water PV separation performance using zeolite membranes

Zeolite	Support	x_{EtOH} (wt%)	y_{EtOH} (wt%)	T (K)	$\beta_{EtOH/water}$	F (kg m^{-2} h^{-1})	F (L m^{-2} h^{-1})	Contact angle (°)	Energy consumption (kJ g^{-1})	P_{EtOH}/l (GPU)	$\alpha_{EtOH/water}$	Ref.
M1[a]	α-Al_2O_3	16	96	348	145	0.36	0.45	NR[e]	NR	110.80	8.40	[45]
M2[b]	α-Al_2O_3	16	97	360	204	0.19	0.24	NR	NR	36.51	11.30	[45]
M2c[c]	α-Al_2O_3	16	95	373	107	0.57	0.71	NR	NR	65.98	6.60	[45]
Silicalite-1	SS	5.0	35	298	10.0	0.07	0.08	NR	11.83	159.03	0.25	[47]
Al-ZSM-5	SS	5.0	33	298	9.40	0.06	0.06	NR	12.54	128.52	0.23	[47]
Fe-ZSM-5	SS	5.0	15	298	3.40	0.06	0.06	NR	33.15	58.42	0.08	[47]
B-ZSM-5	SS	5.0	10	298	2.10	0.05	0.05	NR	53.14	32.45	0.05	[47]
Ge-ZSM-5	SS	5.0	60	298	29.0	0.11	0.13	NR	4.64	428.40	0.70	[47]
Silicalite	SS	4.4	71	303	58.2	0.22	0.26	NR	NR	828.06	1.30	[54]
ZSM-5	Al_2O_3	4.4	18	303	5.20	0.19	0.20	NR	NR	181.30	0.10	[54]
B-ZSM-5	α-Al_2O_3 coated SiC	5.0	62	333	31.0	0.16	0.18	NR	4.40	104.90	0.80	[55]
Silicalite	α-Al_2O_3	5.0	82	333	89.0	1.80	2.18	NR	NR	1,561.00	2.45	[57]
Silicalite	Mullite	5.0	85	333	106	0.90	1.10	NR	NR	809.30	3.05	[58]
Silicalite	α-Al_2O_3	5.0	82	333	85.0	1.22	1.48	NR	NR	1,058.00	2.45	[58]
Silicalite[d]	Mullite	5.0	77	333	65.0	1.28	1.53	NR	NR	1,042.00	1.80	[58]
Silicalite	Silica	3.0	68	353	66.0	1.49	1.74	NR	3.69	16.82	4.40	[59]

[a]Calcined MFI membrane; [b]Ozonicated MFI membrane; [c]Calcined MFI membrane after ozonication; [d]Fabricated by seeded method; [e]Not reported

Finally, the energy consumption to evaporate permeate in a pervaporation process, normalized per unit of EtOH permeated, (Q_{norm}^{evap}, kJ g^{-1}) was also calculated as Eq. (7) when the feed volume was reported [44].

$$Q_{norm}^{evap} = H_{EtOH}^{evap} + H_{water}^{evap}\left(\frac{C_{water}^{feed}}{\beta_{EtOH/water} C_{EtOH}^{feed}}\right) \quad (7)$$

where H_{EtOH}^{evap} and H_{water}^{evap} are the heat of evaporation of EtOH and water, 0.854 and 2.26 kJ g^{-1}, respectively; C_{EtOH}^{feed} and C_{water}^{feed} are the molar concentration of EtOH and water in mole m^{-3}; and $\beta_{EtOH/water}$ is separation factor of EtOH over water.

Next, the permeance and selectivity of each membrane were plotted in Fig. 5, which presents the well-known upper bound relationship for membrane separation introduced by Robeson [60,61]. Since the performance of membranes is governed by a trade-off between permeance and selectivity, future PV membrane research should be focused on surpassing this upper bound. Among reported zeolite PV membranes for EtOH/water separation, MFI membrane on α-Al_2O_3 activated by a ozonication, M2 membrane, and a silicalite membrane on α-Al_2O_3, exhibited the highest selectivity and permeance, respectively. Therefore, the pore activation method as well as the type of zeolite used highly affect the final performance of the membranes.

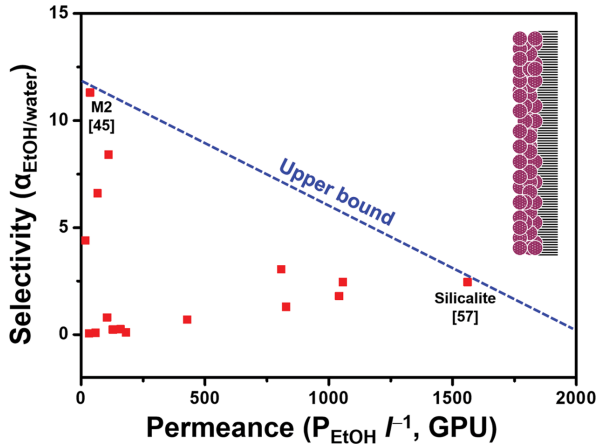

Fig. 5. Upper bound correlation for EtOH/water separation using zeolite membranes. Data were taken from references [45,47, 54,55,57-59].

2. Functionalized Mesoporous Silica Membranes

Porous silica offers several advantages over other inorganic materials for the purpose of membrane separation. First, silica membranes consisting of a porous structure allow small molecules to pass through the pore channels [62]. Moreover, the pore size can be controlled by selecting an appropriate surfactant during synthesis, because the carbon chain length of the surfactant determines the final pore size. Further, the silica surface can be modified by functional groups to tailor the specific selective properties for the target component while losing the high permeation due to the reduced effective pore size caused by the functionalization agent. Due to the aforementioned advantages, porous silica membranes have received attention for the application of PV to separate EtOH [63].

Generally, pristine porous silica is hydrothermally unstable because the surface is hydrophilic owing to the abundant hydroxyl groups (-OH) which preferentially adsorb water [64]. This hydrophilic nature of porous silica membranes means they are better suited to the separation of water from EtOH rich solution, but substantially limits their application for EtOH recovery from aqueous solution. Thus, microporous (<2 nm) silica membrane is more desirable for water permeating, than mesoporous (2-50 nm) silica membrane that can be applied in EtOH permeating after functionalization,

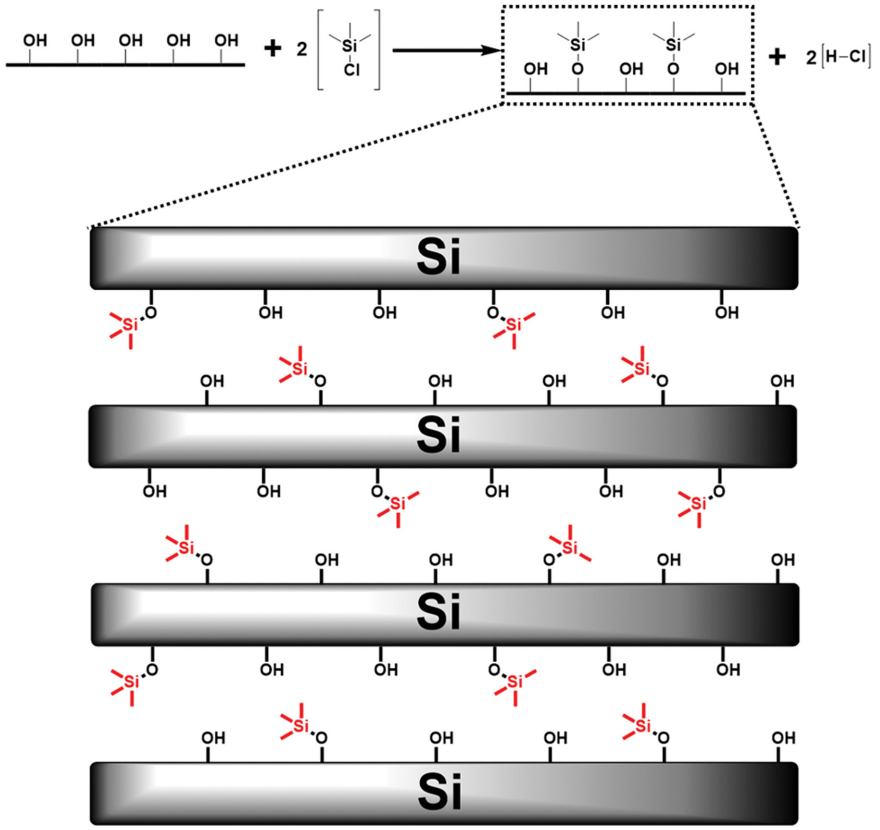

Fig. 6. The silylation process using trimethylchlorosilane and its effect on the mesopore structure of silica membrane.

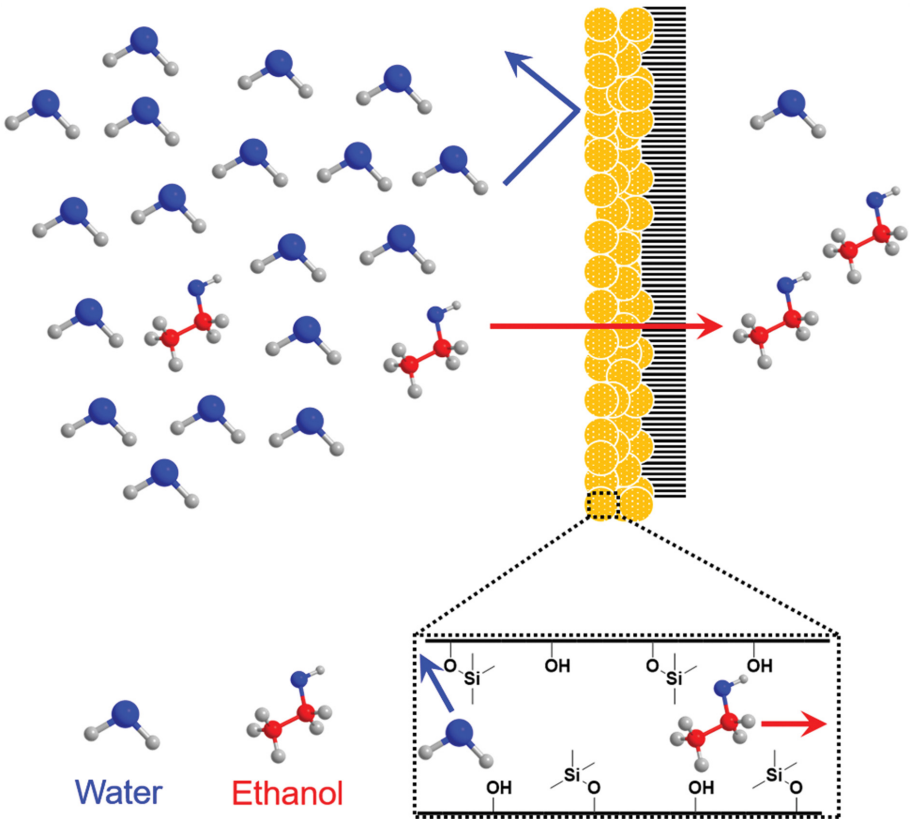

Fig. 7. The proposed mechanism for the PV separation of EtOH/water mixture by silylated mesoporous silica membranes.

because the relatively larger pore size provides more opportunity for modification even though losing some throughput. To tailor the hydrophobicity on the mesoporous silica membranes, surface hydroxyl groups have been functionalized by various methods [65], and silylation is a well-known functionalization method [66]. Fig. 6 shows the silylation process using trimethylchlorosilane at the molecular level and its effect on the pore structure of mesoporous silica membranes.

Silylated mesoporous silica membranes can be applied to the recovery of EtOH as PV process, and the transport mechanism is governed by solution-diffusion as illustrated in Fig. 7. Generally, the separation performance is governed by the rate and degree of dissolution into the membrane surface [67]. Also, the diffusivity between the components, here EtOH and water, affects the separation performance of a membrane [68]. Park et al. prepared MCM-48, cubic member of the M41S family which has a 3-D interconnected mesoporous structure, membranes on porous α-Al_2O_3 supports, then further silylated using trimethylsilane (TM) and triethylsilane (TE) [69]. PV separation performance was evaluated for 10 wt% EtOH/water at 293 K. As a baseline, a pristine MCM-48 membrane exhibited a separation factor of 0.3 with high flux of 16.74 kg m^{-2} h^{-1}, indicating the hydrophilic nature of mesoporous silica membranes. However, the TM- and TE-MCM-48 membranes displayed a separation factor of 13 and 24, respectively, corresponding to 53 and 80 times higher than that of the pristine MCM-48 membrane, whereas significant loss on total flux to 0.3 and 0.06 kg m^{-2} h^{-1}, respectively, because the pore functionalization reduces the effective diffusivity of silylated membranes. There is no significant difference in pore size between TM- and TE-MCM-48, but compared with the nonsilylated membrane, the pore size was reduced from 2.4 nm to 1.9 nm (TM-MCM-48) and 1.8 nm (TE-MCM-48). This result probably contributed to enhancement of separation performance for the silylated membrane. Moreover, no difference in Brunauer-Emmett-Teller surface area before and after silylation indicates the silyl group uniformly functionalized on the surface of the membrane. Further, the difference in separation performance for TM- and TE-MCM-48 cannot be addressed because of presumably different physical properties of the membranes, such as effective pore size and amine loading. Although there is no scientific discussion regarding the effect of different silylation agents, silylation is a useful method to improve the separation performance of mesoporous silica membranes.

On the other hand, even though MCM-48 facilitates efficient transport without any alignment issue, cracks and pinholes, arising during synthesis and surfactant removal due to discontinuity of the structure or thermal expansion, are a serious challenge [70]. To avoid the development of cracks and pinholes during membrane synthesis, Kim et al. synthesized MCM-48 membranes on an α-Al_2O_3 support via a seeded growth method, frequently used for defect-free zeolite membrane fabrication [71]. The pores of the MCM-48 membrane were activated by calcination and further silylated using hexamethyldisilazane. Since the silylation treatment converted pore surface silanol groups to trimethylsilyl groups, the hydrophobicity was increased while decreasing in total flux. Then, they applied pristine and silylated MCM-48 membranes to separate organic/water mixtures such as EtOH, methyl ethyl ketone, and ethyl acetate at 303 K. For the EtOH separation, the separation factor increased from 0.69 to 6.20, which indicates that the silylated membrane was selective for EtOH molecules. At a higher temperature like 343 K, the separation factor enhancement (from 0.51 to 3.03) is relatively low, because permeability of silylated MCM-48 is more highly dependent on adsorption of the components into the mesopores (which decreases with increasing temperature) rather than diffusivity in the mesopores (which increases with temperature). Additionally, the flux was decreased as the separation factor increased, because the enhancement of hydrophobicity selectively retentates water molecules. Further, Kim et al. also developed the silica membrane with worm-like mesoporous structures on Torlon® (polyamide-imide) hollow fiber supports to expand the configuration from a flat disk to a cylinder, which enables compact modules with a high membrane surface area (>1,000 m^2 m^{-3}) [72]. When this cylindrical membrane was applied to PV to separate EtOH from a 5 wt% EtOH/water at 303 K, the separation factor was 4.14 and the EtOH flux was 0.18 kg m^{-2} h^{-1}. This selective and high-flux separation is attributed to both the organophilic nature of the modified mesopores and the large effective pore size even after func-

Table 2. EtOH/water PV separation performance using functionalized mesoporous silica membranes

Functionalized mesoporous silica	Support	x_{EtOH} (wt%)	y_{EtOH} (wt%)	T (K)	$\beta_{EtOH/water}$	F (kg m^{-2} h^{-1})	F (L m^{-2} h^{-1})	Contact angle (°)	Energy consumption (kJ g^{-1})	P_{EtOH}/l (GPU)	$\alpha_{EtOH/water}$	Ref.
MCM-48	α-Al_2O_3	10	3.2	293	0.30	16.740	16.90	NR[d]	NR	3,338	0.010	[69]
TM[a]-MCM-48	α-Al_2O_3	10	64	293	16.00	0.300	0.35	NR	NR	1,196	0.660	[69]
TE[b]-MCM-48	α-Al_2O_3	10	73	293	24.00	0.060	0.07	NR	NR	272.0	1.000	[69]
MCM-48	α-Al_2O_3	5	3.5	303	0.69	0.450	0.45	NR	NR	70.00	0.015	[71]
MCM-48	α-Al_2O_3	5	2.6	343	0.51	0.790	0.80	NR	NR	13.40	0.013	[71]
Silylated[c] MCM-48	α-Al_2O_3	5	25	303	6.20	0.093	0.10	NR	NR	115.0	0.170	[71]
Silylated[c] MCM-48	α-Al_2O_3	5	14	343	3.03	0.150	0.15	NR	NR	14.00	0.080	[71]
Worm-like silica	Torlon® hollow fiber	5	4.8	303	0.95	3.240	3.28	NR	NR	1,663	0.050	[72]
Worm-like silica	Torlon® hollow fiber	5	6.4	323	1.30	6.700	6.81	NR	NR	1,494	0.070	[72]
Silylated[c] worm-like silica	Torlon® hollow fiber	5	18	303	4.14	0.960	1.00	NR	NR	2,317	0.310	[72]
Silylated[c] worm-like silica	Torlon® hollow fiber	5	19	323	4.59	3.100	3.24	NR	NR	2,461	0.290	[72]

[a]Trimethylsilane functionalized; [b]Triethylsilane functionalized; [c]Hexamethyldisilazane functionalized; [d]Not reported

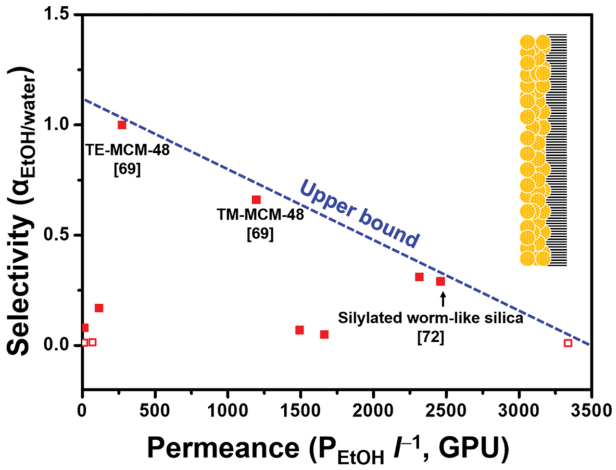

Fig. 8. Upper bound correlation for EtOH/water separation using mesoporous silica membranes. Data were taken from references [45,69,71,72] (Filled square: functionalized mesoporous silica membrane, unfilled square: mesoporous silica membrane).

tionalization. More importantly, the present membranes are promising due to the use of scalable and low-cost supports and good separation performance. A comparison with their flat silylated MCM-48 membrane on an α-Al_2O_3 support [71], the worm-like mesoporous silica membrane fabricated on polymeric hollow fiber, further silylated, has a higher flux and greater selectivity. Thus, silylation affects to increase the separation factor of EtOH followed by enhanced hydrophobicity of the membrane, but also decreases the total flux, especially water flux, because of reduced effective pore size of the membranes.

Like zeolite membranes, the reported EtOH/water PV separation performances of functionalized mesoporous silica membranes were summarized with the same format in Table 2 and an upper bound correlation was plotted in Fig. 8. The unfilled points indicate non-functionalized mesoporous silica membranes. The performances of the TE-MCM-48, TM-MCM-48, and silylated worm-like silica membranes were located near the upper bound, exhibiting a better separation property than the other functionalized mesoporous silica membranes. From the given trade-off between membranes, the order of hydrophobicity is implied as TE-MCM-48> TM-MCM-48>silylated worm-like silica membranes, which can be proportional to the loading of silylation agent. On the other hand, the permeance of those membranes is the reverse order, presumably attributed to the effective pore size of each functionalized membrane. Thus, appropriate loading of silylation agent to tailor hydrophobicity and pore size after silylation determine the performance of functionalized mesoporous silica membranes, indicating that the development of functionalization technique will establish superior performance to overcome the shown upper bound.

3. Mixed Matrix Membranes

To harness the advantages of both inorganic and organic materials, a technique to incorporate inorganic fillers into the polymer framework is adopted, forming so called MMMs [73]. In the fabrication of MMMs, it is very important to find an appropriate loading of inorganic fillers to maximize the PV performance and enhance the affinity between the inorganic fillers and the polymer to minimize voids in the interface [74]. Further, ensuring a homogeneous dispersion of the inorganic filler throughout the polymer matrix is a particularly important challenge [75]. Polydimethylsiloxane (PDMS) is widely used to fabricate hydrophobic PV membranes with incorporation of inorganic fillers because of its fairly good chemical resistance, high permeability, and intrinsic hydrophobic properties [76]. For the inorganic filler, a hydrophobicity tailored zeolite or metal organic framework (MOF) is frequently hired to fabricate MMMs. Liu et al. synthesized MMM by homogeneously dispersing silylated ZSM-5 in a PDMS matrix [77]. First, commercial ZSM-5 is grafted with *n*-octyltriethoxysilane to increase hydrophobicity and homogeneously dispersed into the PDMS matrix via a newly developed surface graft approach. The grafted silane group on the zeolite surface entangles with PDMS, which greatly improves the affinity between zeolite particles and the PDMS matrix. Diverse zeolite loading ranging from 10 wt% to 40 wt% was tried and a higher separation factor and lower flux were obtained as zeolite loading increased. The reported separation factor and flux were 14 and 0.40 kg m^{-2} h^{-1}, respectively, when applying 40 wt% silylated ZSM-5 MMM for a 5 wt% EtOH/water at 313 K. Considering permeance, higher loading of silylated ZSM-5 significantly reduces the permeance of water, thereby increasing selectivity.

Yi et al. synthesized MMM with vinyltriethoxysilane (VTES) modified silicalite-1 and PDMS [78]. The VTES group chemically bonded to the surface of silicalite-1 without any influence on crystal structure, and hence suppressed the formation of microvoids at the silicalite-1 and PDMS interface. This is because vinyl groups on the surface of modified silicalite-1 reacted with cross-linked and prepolymer of PDMS, thereby forming dense cross-linked polymer networks through the Pt-catalyzed hydrosilylation reaction. Diverse loadings of pristine and modified silicalite-1 were incorporated into PDMS and tested for 5 wt% EtOH/water at temperatures ranging from 303 K to 338 K. Similarly, higher separation factors as well as lower total flux were achieved as silicalite-1 loading increased from 0 to 60 wt%. Compared to the pristine silicalite-1/PDMS membrane applied PV to the 5 wt% EtOH/water at 323 K, modified MMM has reduced water flux and thereby a significantly enhanced separation factor. The best PV performance, when 67 wt% of modified silicalite-1 was incorporated into the PDMS matrix, indicates a separation factor and flux of 32 and 0.091 kg m^{-2} h^{-1}. Also, the selectivity was enhanced from 0.53 (MMM with 60 wt% pristine silicalite-1) to 0.8 (MMM with 67 wt% modified silicalite-1).

If the inorganic filler has a hollow sphere (HS) shape, it creates pathways for molecular transport lowering mass transfer resistance. Naik et al. developed PDMS based MMMs containing HS covered with silicalite-1 and investigated their PV performance on 5 wt% EtOH/water [79]. The 1 μm sized HS was prepared by a surfactant templating method, then covered with a thin shell of silicalite-1 crystals. As HS loading increased up to 30 wt%, an increase in flux and selectivity for EtOH was obtained. Further, comparison with silicalite-1/PDMS MMM exemplifies that HS plays quite an important role for enhanced EtOH permeance. Since the HS provides a pathway for molecular transport while decreasing the mass transfer resistance, the EtOH permeates through the membrane as a selectively sorbed component. Moreover, evenly dispersed HS in

Table 3. EtOH/water PV separation performance using MMMs

Inorganic filler	Inorganic loading (wt%)	Polymer matrix	x_{EtOH} (wt%)	y_{EtOH} (wt%)	T (K)	$\beta_{EtOH/water}$	F (kg m^{-2} h^{-1})	F (L m^{-2} h^{-1})	Contact angle (°)	Energy consumption (kJ g^{-1})	P_{EtOH}/l (GPU)	$\alpha_{EtOH/water}$	Ref.
ZSM-5[a]	10	PDMS	5	30.40	313	8.3	1.750	1.87	118	NR	245.0	0.78	[77]
ZSM-5[a]	20	PDMS	5	32.14	313	9.0	0.950	1.02	121	NR	182.0	0.85	[77]
ZSM-5[a]	30	PDMS	5	36.67	313	11.0	0.700	0.76	128	NR	179.0	1.03	[77]
ZSM-5[a]	40	PDMS	5	42.42	313	14.0	0.410	0.45	139	NR	203.0	1.32	[77]
Silicalite-1	60	PDMS	5	52.50	323	21.0	0.108	0.12	NR[f]	6.08	95.2	0.53	[78]
Silicalite-1[b]	60	PDMS	5	57.78	323	26.0	0.099	0.11	NR	5.08	95.6	0.65	[78]
Silicalite-1[b]	67	PDMS	5	62.75	323	32.0	0.091	0.11	NR	4.29	95.6	0.80	[78]
Silicalite-1	30	PDMS	6	48.75	313	14.9	0.050	0.06	NR	NR	186.8	1.10	[79]
Silicalite-1 covered HS[c]	30	PDMS	6	49.41	313	15.3	0.070	0.08	NR	NR	260.2	1.30	[79]
MAF-6	15	PDMS	5	43.95	313	14.9	1.200	1.33	120	NR	342.3	0.58	[80]
CNT[d]-GO[e]	0.75	PDMS	5	54.22	305	22.5	0.22	0.25	126	NR	524.9	0.26	[81]

[a]*n*-Octyltriethoxysilane functionalized; [b]Vinyltriethoxysilane functionalized; [c]Hollow sphere; [d]Carbon nanotube; [e]Graphene oxide; [f]Not reported

the PDMS matrix and fairly good adhesion between HS and PDMS benefit the enhanced performance of this MMM.

Li et al. fabricated a hydrophobic MMM by incorporation of RHO-[$Zn(eim)_2$] (MAF-6), one of the MOFs, into PDMS [80]. MAF-6 is an exceptionally hydrophobic MOF, both in internal pores and external crystal surfaces, with high thermal/chemical stability and exhibits a relatively large pore size (~1.84 nm). Different from previously described MMMs, the separation factor of MAF-6 incorporated MMM increased up to 15 wt% of MOF loading, and then dropped with further increase of the loading. On the other hand, significant increase of flux is probably due to the microdefects at the interface between MAF-6 and PDMS matrix. Moreover, the decreased contact angle of 20 wt% and 25 wt% MAF-6 loading MMMs supported reduced hydrophobicity. Also, increased MAF-6 loading over 15 wt% leads to defects. The best separation performance of an MMM with 15 wt% MAF-6 loading was a separation factor of 14.9 and flux of 1.2 kg m^{-2} h^{-1}, which was 1.5 times and 2.3 times higher than pristine PDMS membrane on the PV of 5 wt% EtOH/water at 313 K. Such extraordinary separation performance is attributed to the superior adsorption ability of MAF-6 for EtOH over water. Recently, the carbon nanotube (CNT)-coupled graphene oxide (GO) incorporated, ranging from 0.25 to 1 wt%, into PDMS framework to separate EtOH/water solution [81]. When 0.75 wt% was loaded, the best performance in separation factor of 22.5 with flux of 0.22 kg m^{-2} h^{-1} at 305 K. This properly dispersed CNT-coupled-GO-incorporated membrane applied to the long term (~44 h) and large scale operation of EtOH production.

For completeness, the collated data and their upper bound correlation of hydrophobic MMMs for EtOH/water PV separation are presented in Table 3 and Fig. 9. Different from the zeolite and functionalized mesoporous silica membranes, the performance of MMMs is somewhat clustered, implying that both permeance and selectivity diverge over a very short range. Among given MMMs, the silicalite-1 covered HS incorporated in a PDMS matrix exhibited the superior performance, which indicates the structure of inorganic filler affects the quality of the MMM. On the other hand, MMM with CNT-GO presented the highest permeance and relatively low selectivity. This is due to the thin layer and limited loadings (0.25-1 wt%) of CNT-GO. Thus, a fairly good MMM is supposed to possess good affinity between polymer matrix and inorganic fillers with high selectivity for EtOH. Further, the inorganic filler should be well functionalized with an appropriate agent before forming a membrane. Moreover, homogeneous dispersion of the inorganic filler in the polymer matrix is also important to provide high loading on a thin membrane layer.

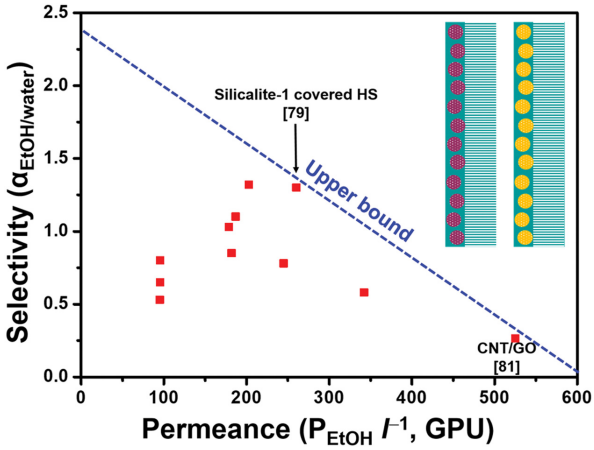

Fig. 9. Upper bound correlation for EtOH/water separation using MMMs. Data were taken from references [77-81].

OUTLOOK

Fig. 10 summarizes all three different upper bound relationships regarding inorganic hydrophobic PV membrane separation for EtOH/water shown in Figs. 5, 8, and 9. Comprehensively, the order of selectivity is zeolite>MMM>functionalized mesoporous silica, corresponding to the order of y-intercepts in upper bound correlation. While the permeance is of the order of functionalized mesoporous silica>MMM>zeolite, coinciding with the order of slopes. This informs the PV membrane community that zeolite mem-

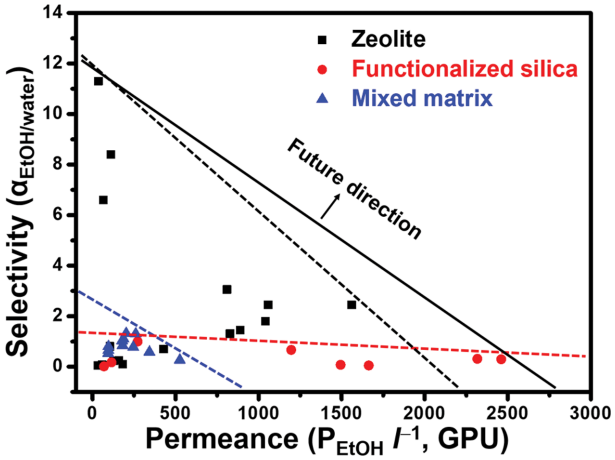

Fig. 10. Upper bound correlation for EtOH/water separation using zeolite, functionalized mesoporous silica, and MMMs.

branes have a challenge to improve the permeance, whereas the functionalized mesoporous silica membranes are required to enhance selectivity, which can be potentially achieved by elucidating the pore structure and fabricated membrane orientation of zeolite and developing better functionalization techniques on mesoporous silica, respectively.

As the scientific community continues to strive towards eco-friendly and sustainable bio-fuel manufacture, PV will play its part [81-84]. Specifically related to EtOH dehydration, many developments continue to be made with hydrophilic PV membranes such as those based on polymers [81,84,85], impregnated polymers [86, 87], MMMs [83,88], and zeolites [89,90]. Such advancements can be applied to, inspire and energize the hydrophobic PV community, particularly in relation to inorganic membranes in the areas of direct characterization of pore structure, loading of functionalization agent, long-term performance stability, dependence of support material, and inorganic filler arrangement.

CONCLUSIONS

EtOH/water separation using hydrophobic PV inorganic membranes is a rapidly growing research field due to future energy requirement and spotlighted by the porous inorganic community. Zeolites, functionalized mesoporous silica, and MMMs exhibit significantly promising PV performance for EtOH/water separation attributed by the intrinsic porosity of the materials and strong surface hydrophobicity. However, there are still unknown territories in each category of materials regarding direct characterization of pore structure, loading of functionalization agent, long term performance stability, dependence of support material, and inorganic filler arrangement. The correlations of those properties with permeation performance in the PV process are going to bring the hydrophobic inorganic membranes to a technologically scalable platform appropriate for direct industrial applications in EtOH recovery.

ACKNOWLEDGEMENT

The authors are grateful for the financial support from National Research Foundation of Korea (NRF) grant funded by the Korea government (MSIP) (No. RS-2022-00155422).

CONFLICT OF INTEREST

The authors declare no conflict of interest.

REFERENCES

1. R. E. H. Sims, W. Mabee, J. N. Saddler and M. Taylor, *Bioresour. Technol.*, **101**, 1570 (2010).
2. M. FitzPatrick, P. Champagne, M. F. Cunningham and R. A. Whitney, *Bioresour. Technol.*, **101**, 8915 (2010).
3. Y. Lin and S. Tanaka, *Appl. Microbiol. Biotechnol.*, **69**, 627 (2006).
4. A. Demirbas, *Energy Convers. Manag.*, **49**, 2106 (2008).
5. S. N. Naik, V. V. Goud, P. K. Rout and A. K. Dalai, *Renew. Sustain. Energy Rev.*, **14**, 578 (2010).
6. S. Kim and B. E. Dale, *Biomass Bioenergy*, **26**, 361 (2004).
7. A. Gupta and J. P. Verma, *Renew. Sustain. Energy Rev.*, **41**, 550 (2015).
8. C. Cannilla, G. Bonura and F. Frusteri, *Catalysts*, **7**, 187 (2017).
9. N. I. S. Muhammad and K. A. Rosentrater, *Energies*, **13**, 436 (2020)
10. J. R. Kwiatkowski, A. J. McAloon, F. Taylor and D. B. Johnston, *Ind. Crops Prod.*, **23**, 288 (2006).
11. K. Ueno, H. Negishi, M. Miyamoto, S. Uemiya and Y. Oumi, *Micropor. Mesopor. Mater.*, **267**, 1 (2018).
12. L. M. Vane and F. R. Alvarez, *J. Chem. Technol. Biotechnol.*, **90**, 1380 (2015).
13. B. P. Tripathi, M. Kumar, A. Saxena and V. K. Shahi, *J. Colloid Interface Sci.*, **346**, 54 (2010).
14. P. D. Chapman, T. Oliveira, A. G. Livingston and K. Li, *J. Membr. Sci.*, **318**, 5 (2008).
15. H. Zheng and M. Yoshikawa, *J. Membr. Sci.*, **478**, 148 (2015).
16. H. A. Tsai, H. C. Chen, W. L. Chou, K. R. Lee, M. C. Yang and J. Y. Lai, *J. Appl. Polym. Sci.*, **94**, 1562 (2004).
17. H.-J. Huang, S. Ramaswamy, U. W. Tschirner and B. V. Ramarao, *Sep. Purif. Technol.*, **62**, 1 (2008).
18. P. Peng, B. Shi and Y. Lan, *Sep. Sci. Technol.*, **46**, 234 (2011).
19. P. Wei, L. H. Cheng, L. Zhang, X. H. Xu, H. L. Chen and C. J. Gao, *Renew. Sustain. Energy Rev.*, **30**, 388 (2014).
20. X. Feng and R. Y. M. Huang, *Ind. Eng. Chem. Res.*, **36**, 1048 (1997).
21. H. Saleem and S. J. Zaidi, *Desalination*, **475**, 114171 (2020).
22. P. S. Goh and A. F. Ismail, *Desalination*, **434**, 60 (2018).
23. S. L. Wee, C. T. Tye and S. Bhatia, *Sep. Purif. Technol.*, **63**, 500 (2008).
24. P. S. Goh and A. F. Ismail, *J. Chem. Technol. Biotechnol.*, **90**, 971 (2015).
25. K. Katsoufidou, S. G. Yiantsios and A. J. Karabelas, *J. Membr. Sci.*, **266**, 40 (2005).
26. A. W. Mohammad, Y. H. Teow, W. L. Ang, Y. T. Chung, D. L. Oatley-Radcliffe and N. Hilal, *Desalination*, **356**, 226 (2015).
27. K. P. Lee, T. C. Arnot and D. Mattia, *J. Membr. Sci.*, **370**, 1 (2011).
28. T. S. Chung, S. Zhang, K. Y. Wang, J. Su and M. M. Ling, *Desalination*, **287**, 78 (2012).
29. W. L. Luyben, *Ind. Eng. Chem. Res.*, **48**, 3484 (2009).
30. R. W. Baker, *Membrane technology and applications*, John Wiley & Sons, Ltd, UK (2004).
31. M. M. Reyes Mallada, *Inorganic membranes: synthesis, characteri-*

zation and applications, Elsevier (2008).
32. W. F. Guo, T. S. Chung and T. Matsuura, *J. Membr. Sci.*, **245**, 199 (2004).
33. R. W. Baker, J. G. Wijmans and Y. Huang, *J. Membr. Sci.*, **348**, 346 (2010).
34. S. D. Bhat, B. V. K. Naidu, G. V. Shanbhag, S. B. Halligudi, M. Sairam and T. M. Aminabhavi, *Sep. Purif. Technol.*, **49**, 56 (2006).
35. M. Moliner, C. Martínez and A. Corma, *Chem. Mater.*, **26**, 246 (2014).
36. Z. Lai, G. Bonilla, I. Diaz, J. G. Nery, K. Sujaoti, M. A. Amat, E. Kokkoli, O. Terasaki, R. W. Thompson, M. Tsapatsis and D. G. Vlachos, *Science*, **300**, 456 (2003).
37. H. Kita, K. Horii, Y. Ohtoshi, K. Tanaka and K. I. Okamoto, *J. Mater. Sci. Lett.*, **14**, 206 (1995).
38. J. C. Tan, T. D. Bennett and A. K. Cheetham, *Proc. Natl. Acad. Sci. U.S.A.*, **107**, 9938 (2010).
39. N. Rangnekar, N. Mittal, B. Elyassi, J. Caro and M. Tsapatsis, *Chem. Soc. Rev.*, **44**, 7128 (2015).
40. M. E. Ersahin, H. Ozgun and J. B. van Lier, *Sep. Sci. Technol.*, **48**, 2263 (2013).
41. B. Achiou, D. Beqqour, H. Elomari, A. Bouazizi, M. Ouammou, M. Bouhria, A. Aaddane, K. Khiat and S. Alami Younssi, *J. Environ. Chem. Eng.*, **6**, 4429 (2018).
42. T. Mohammadi and A. Pak, *Sep. Purif. Technol.*, **30**, 241 (2003).
43. W. Liu, J. Zhang, N. Canfield and L. Saraf, *Ind. Eng. Chem. Res.*, **50**, 11677 (2011).
44. L. M. Vane, *J. Chem. Technol. Biotechnol.*, **80**, 603 (2005).
45. J. Kuhn, S. Sutanto, J. Gascon, J. Gross and F. Kapteijn, *J. Membr. Sci.*, **339**, 261 (2009).
46. J. Kuhn, M. Motegh, J. Gross and F. Kapteijn, *Micropor. Mesopor. Mater.*, **120**, 35 (2009).
47. V. A. Tuan, S. Li, J. L. Falconer and R. D. Noble, *J. Membr. Sci.*, **196**, 111 (2002).
48. L. S. M. Nazir, Y. F. Yeong and T. L. Chew, *J. Asian Ceram. Soc.*, **8**, 553 (2020).
49. X. Xu, Y. Bao, C. Song, W. Yang, J. Liu and L. Lin, *Micropor. Mesopor. Mater.*, **75**, 173 (2004).
50. T. Mohammadi and A. Pak, *Micropor. Mesopor. Mater.*, **56**, 81 (2002).
51. W. C. Wong, L. T. Y. Au, C. T. Ariso and K. L. Yeung, *J. Membr. Sci.*, **191**, 143 (2001).
52. V. A. Tuan, J. L. Falconer and R. D. Noble, *Ind. Eng. Chem. Res.*, **38**, 3635 (1999).
53. S. Li, V. A. Tuan, R. D. Noble and J. L. Falconer, *Ind. Eng. Chem. Res.*, **40**, 6165 (2001).
54. T. Sano, S. Ejiri, K. Yamada, Y. Kawakami and H. Yanagishita, *J. Membr. Sci.*, **123**, 225 (1997).
55. T. C. Bowen, H. Kalipcilar, J. L. Falconer and R. D. Noble, *J. Membr. Sci.*, **215**, 235 (2003).
56. M. Nomura, T. Bin and S. I. Nakao, *Sep. Purif. Technol.*, **27**, 59 (2002).
57. X. Lin, H. Kita and K. I. Okamoto, *Ind. Eng. Chem. Res.*, **40**, 4069 (2001).
58. X. Lin, X. Chen, H. Kita and K. Okamoto, *AIChE J.*, **49**, 237 (2003).
59. H. Chen, Y. Li and W. Yang, *J. Membr. Sci.*, **296**, 122 (2007).
60. L. M. Robeson, *J. Membr. Sci.*, **62**, 165 (1991).
61. L. M. Robeson, *J. Membr. Sci.*, **320**, 390 (2008).
62. H. R. Lee, T. Shibata, M. Kanezashi, T. Mizumo, J. Ohshita and T. Tsuru, *J. Membr. Sci.*, **383**, 152 (2011).
63. S. Araki, S. Imasaka, S. Tanaka and Y. Miyake, *J. Membr. Sci.*, **380**, 41 (2011).
64. Z. Wang, L. Hao, F. Yang and Q. Wei, *Membranes*, **10**, 70 (2020).
65. Q. Wei, Y. L. Ding, Z. R. Nie, X. G. Liu and Q. Y. Li, *J. Membr. Sci.*, **466**, 114 (2014).
66. K. A. Koyano, T. Tatsumi, Y. Tanaka and S. Nakata, *J. Phys. Chem. B*, **101**, 9436 (1997).
67. W. Kujawski and R. Roszak, *Sep. Sci. Technol.*, **37**, 3559 (2002).
68. W. Kujawski, J. Kujawa, E. Wierzbowska, S. Cerneaux, M. Bryjak and J. Kujawski, J. *Membr. Sci.*, **499**, 442 (2016).
69. D. H. Park, N. Nishiyama, Y. Egashira and K. Ueyama, *Ind. Eng. Chem. Res.*, **40**, 6105 (2001).
70. M. Kaneda, T. Tsubakiyama, A. Carlsson, Y. Sakamoto, T. Ohsuna, O. Terasaki, S. H. Joo and R. Ryoo, *J. Phys. Chem. B*, **106**, 1256 (2002).
71. H. J. Kim, K. S. Jang, P. Galebach, C. Gilbert, G. Tompsett, W. C. Conner, C. W. Jones and S. Nair, *J. Membr. Sci.*, **427**, 293 (2013).
72. H. J. Kim, N. A. Brunelli, A. J. Brown, K. S. Jang, W. G. Kim, F. Rashidi, J. R. Johnson, W. J. Koros, C. W. Jones and S. Nair, *ACS Appl. Mater. Interfaces*, **6**, 17877 (2014).
73. H. Vinh-Thang and S. Kaliaguine, *Chem. Rev.*, **113**, 4980 (2013).
74. H. Ren, J. Jin, J. Hu and H. Liu, *Ind. Eng. Chem. Res.*, **51**, 10156 (2012).
75. A. K. Zulhairun and A. F. Ismail, *J. Membr. Sci.*, **468**, 20 (2014).
76. S. Xu, H. Zhang, F. Yu, X. Zhao and Y. Wang, *Sep. Purif. Technol.*, **206**, 80 (2018).
77. G. Liu, F. Xiangli, W. Wei, S. Liu and W. Jin, *Chem. Eng. J.*, **174**, 495 (2011).
78. S. Yi, Y. Su and Y. Wan, *J. Membr. Sci.*, **360**, 341 (2010).
79. P. V. Naik, S. Kerkhofs, J. A. Martens and I. F. J. Vankelecom, *J. Membr. Sci.*, **502**, 48 (2016).
80. Q. Li, L. Cheng, J. Shen, J. Shi, G. Chen, J. Zhao, J. Duan and G. Liu, *Sep. Purif. Technol.*, **178**, 105 (2017).
81. S. Shafiei Amrei, M. Asghari, M. Esfahanian and Z. Zahraei, *J. Chem. Technol. Biotechnol.*, **95**, 1604 (2020).
82. A. Çalhan, S. Deniz, J. Romero and A. Hasanoğlu, *Korean J. Chem. Eng.*, **36**, 1489 (2019).
83. P. Mizsey, A. Selim, A. J. Toth, D. Fozer and K. Süvegh, *ACS Omega*, **5**, 32373 (2020).
84. A. S. Kulkarni, A. M. Sajjan, M. Ashwini, N. R. Banapurmath, N. H. Ayachit and G. G. Shirnalli, *RSC Adv.*, **10**, 22645 (2020).
85. P. Grzybek, Ł. Jakubski, P. Borys, S. Kołodziej, C. Ślusarczyk, R. Turczyn and G. Dudek, *Sep. Purif. Technol.*, **281**, 119897 (2022).
86. G. Dudek, R. Turczyn and D. Djurado, *Materials*, **13**, 4152 (2020).
87. F. Pan, C. Cao, G. Liu and Z. Jiang, *Chem. Eng. Sci. X*, **11**, 100102 (2021).
88. R. Castro-Muñoz and G. Boczkaj, *Molecules*, **26**, 1242 (2021).
89. Y. Hasegawa, C. Abe and A. Ikeda, *Membranes*, **11**, 229 (2021).
90. L. Li, Y. Lu, L. Li, J. Yang, W. Fu, Y. Luo, J. Lu, Y. Zhang and L. Zhou, *J. Membr. Sci.*, **638**, 119701 (2021).